International Journal of Fluid Power 10 (2009) No. 2 pp. 19-28

DESIGN AND CONTROL OF A SHIP MOTION SIMULATION PLATFORM FROM AN ENERGY EFFICIENCY PERSPECTIVE

John Jansen, Randall Lind, Lonnie Love, Peter Lloyd, John Rowe and François G. Pin

Oak Ridge National Laboratory, Oak Ridge, TN, USA
jansenjf@ornl.gov, lovelj@ornl.gov, lindlf@ornl.gov, lloydpd@ornl.gov,rowejc@ornl.gov, pin@ornl.gov

Abstract

Most hydraulic servo systems are designed with little consideration for energy efficiency. Pumps are selected based upon required peak power demands, valves are chosen primarily for their rated flow, actuators for the maximum force. However, the design of a hydraulic servo system has great potential in terms of energy efficiency that has, for the most part, been ignored. This paper describes the design and control of a large-scale ship motion simulation platform that was designed and built at Oak Ridge National Laboratory for the Office of Naval Research. The primary reasons to incorporate energy-efficiency features into the design are cost and size reduction. A preliminary survey of proposed designs based on traditional motion simulation platform configurations (Stewart Platforms) required hydraulic power supplies approaching 1.22 MW. This manuscript describes the combined design and control effort that led to a system with the same performance requirements, however requiring a primary power supply that was less than 100 kW. The objective of this paper is to illustrate alternative design and control approaches that can significantly reduce the power requirements of hydraulic systems and improve the overall energy-efficiency of large-scale hydraulically actuated systems.

Keywords: hydraulics, energy efficiency, ship motion simulation platform, sea states

1 Introduction

The primary focus of this paper is on the design and control of an energy efficient hydraulic servo system simulating wave-induced ship motions for the purpose of testing equipment, such as robotic and human assist devices (Love, 2004), for future use on naval vessels. Testing equipment on a naval vessel introduces many significant logistics and planning problems. The unpredictability of nature makes it extremely difficult to test the system in a variety of sea conditions of interest and essentially impossible to achieve repeatable conditions for accurate evaluations of technologies or to establish a constant baseline for evaluation of different approaches. This provided the motivation for the development of a high fidelity, high payload ship motion simulation platform. Our system, shown in Fig. 1 and 2 has a 2268 kg (5000 lb) payload capacity, five degrees of freedom (heave, surge, sway, pitch and roll), motion capabilities that enable simulation of the wave-induced motions at any point on the ship (currently, models for a Destroyer, Frigate or Aircraft Carrier have been implemented) up to Sea State 5. Sea State refers to a scale used in the Navy to characterize the roughness of the sea, and is mostly based on the height and type of the predominant waves. Figure 3 illustrates the 6-dimensional motions of a typical ship, and Table 1 shows the typical wave height corresponding to several Sea States and the resulting motion parameters of ships of various lengths when submitted to these Sea States.

This manuscript was received on 12 September 2008 and was accepted after revision for publication on 15 May 2009

2 Kinematics and Mechanical Design

2.1 Design Objectives

The objective of the ship motion simulation platform was to develop a system that is capable of providing realistic motion profiles for larger ships (Frigates, Destroyers and Aircraft Carriers) in sea states up to Sea State 5. Most existing motion platforms are for flight or automotive applications which require relatively high frequency, small displacement motions and are based on the Stewart Platform configuration (Lee, 1998; Li, 1997; Tseng, 2005). Ship motion simulation requires relatively low frequency, large displacements and large

Table 1: Ship Response as Function of Sea State

Sea State	Wave Ht (ft)	Boat Length (ft)	Pitch (deg)	Pitch Period (sec)	Heave (ft)	Heave Acc (g)	Beam (ft)	Roll Angle (deg)	Roll Period (sec)
4	6.8	<150	2	3.5	2.2	0.10	<50	7	7.1
		150-250	2	4	2.2	0.10	50-75	6	11.5
		250-350	1	5	2.2	0.10	75-105	6	13.7
		350-500	1	6	1.7	0.08	>105	5	14.8
		500-700	1	7	1.3	0.06			
		>700	1	8	0.9	0.04			
5	9.8	<150	3	3.5	5.2	0.17	<50	12	7.1
		150-250	3	4	5.2	0.17	50-75	10	11.5
		250-350	2	5	5.2	0.17	75-105	10	13.7
		350-500	2	6	4.3	0.14	>105	9	14.8
		500-700	2	7	3.1	0.10			
		>700	1	8	2.1	0.07			
6	17	<150	5	3.5	15.0	0.27	<50	19	7.1
		150-250	4	4	15.0	0.27	50-75	16	11.5
		250-350	4	5	15.0	0.27	75-105	15	13.7
		350-500	3	6	11.7	0.21	>105	13	14.8
		500-700	3	7	8.9	0.16			
		>700	2	8	6.1	0.11			

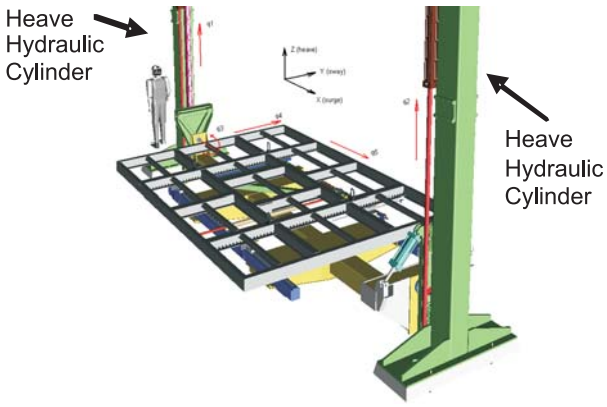

Fig. 1: *SMSP model*

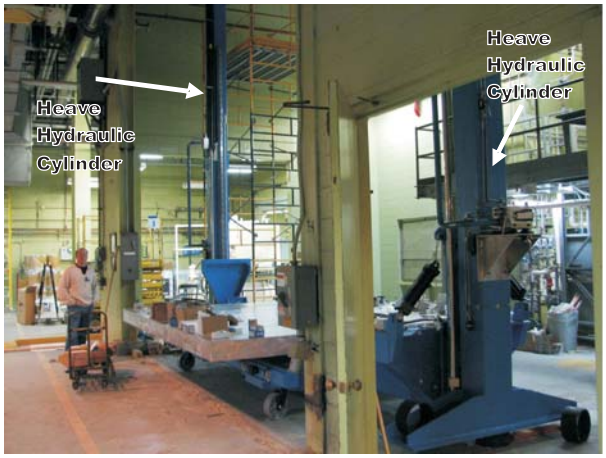

Fig. 2: *SMSP hardware*

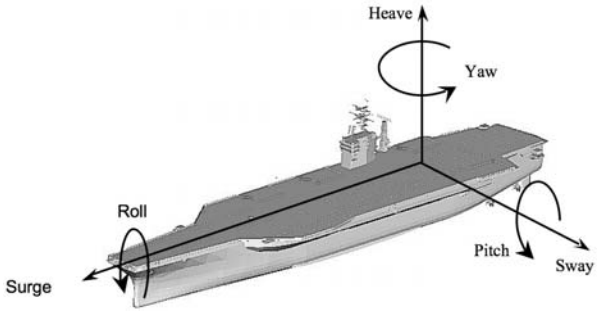

Fig. 3: *Ship displacements*

payload capacity. The system described below has five degrees of freedom (heave, surge, sway, pitch and roll) with 3.0 m of displacement in the heave, 1.2 m of displacement in the sway, 0.6 m of displacement of surge, ±10° of motion in the roll axis and ±2° of pitch motion. The yaw motion was not included due to its insignificant acceleration contribution on large Navy ships. Given the size of the system, tracking accuracy of 6.4 mm and 0.1° were considered acceptable.

Since the purpose of this motion simulator is to generate sea motions that produce realistic inertial forces on test objects, higher sea state motions are possible without needing larger range of motion travel by employing frequency scaling. The frequency content of the motion in all degrees of freedom is generally below 0.5 Hz (typically under 0.2 Hz). Because of the relatively low frequency requirement at the various sea states, the effective forces experienced by test devices on the motion platform could be effectively quadrupled if one would do a time scaling of the motion profile by a factor of 0.5 to effectively double the frequency spectrum of the commanded motion profile.

2.2 Hydraulic Cylinders Configuration

From Table 1, the heave motion provided the dominant displacement and had the greatest power demand (> 10 times all other joints) on the system and will be central to our discussion. Since the sole function of this motion platform is to model sea motion as experienced on naval ships, a very specific kinematic arrangement was utilized to minimize overall energy consumption. In contrast, a conventional Stewart Platform uses six linear actuators in a parallel configuration to provide all six degrees of motion regardless of the power demand requirements. One primary benefit of a Stewart platform is the large vertical stiffness and small moving mass which results in a system with relatively high open-loop bandwidth. The parallel arrangement leads to all six actuators having the same force and speed requirements. Many systems have the actuators located below the platform maintaining the actuator in compression. Sizing of the actuators is based on rod buckling limitations instead of force requirements. Subsequently, the actuators tend to be sized significantly larger than would otherwise be required. An alternative kinematic arrangement is shown in Fig. 1. This system has two parallel heave actuators that are configured in tension to provide the heave and pitch motions. These two actuators provide heave motion through common mode displacement of the two actuators and pitch motion through differential displacement. By placing the actuators in tension, the actuators can be sized for the maximum force requirements instead of rod buckling. This is especially important for systems with the combined high payload and large displacement (the rods must be capable of sustaining 44.5 kN with a maximum displacement of 3.0 m).

The hydraulic natural frequency for these cylinders can be estimated as follows. The cylinders have a bore diameter of 8.3 cm with a 5.1 cm rod diameter (effective area is 33 cm^2). Assuming that the cylinders are at one half of their maximum stroke (1.68 m) and that half the load is seen by each cylinder (22.2 kN), along with an assumed effective fluid bulk modulus of 690 MPa, the approximate hydraulic natural frequency ignoring fluid in the lines is 3.9 Hz. The consequence of this low natural frequency is one of the fundamental limitations in the proposed design and its remedy is discussed in a later section.

Two antagonistic actuators, located on one of the heave actuators, provide the roll motion for the table. Finally, the surge and sway motion are produced by two orthogonal actuators located on the moving table. As mentioned previously, the two heave cylinders are the dominant power loads, and how one reduces their power demand while achieving good tracking performance is the primary focus of this paper.

2.3 Exploiting Gravity

One of the key ideas to further improve energy-efficiency is to utilize gravity to move the heave cylinders down. To accomplish this, the Ship Motion Simulation Platform (SMSP) is designed so that fluid is only controlled on one side of the heave pistons (see Fig. 4) and the other side is vented to tank. When the system is commanded to go vertically up, fluid is throttled from the hydraulic power supply to the cylinder. However, when the system is required to move vertically down, the fluid is only throttled from the cylinder to tank, requiring no power from the hydraulic power supply. This strategy enables controlled motion in both directions while only requiring hydraulic power during positive vertical motions, thereby cutting the overall power requirements for the system in about half.

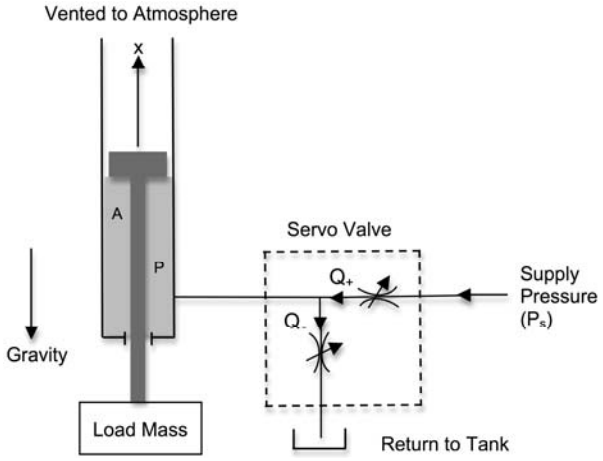

Fig. 4: *Simplified heave mast hydraulic schematic*

2.4 Energy Storage

To further reduce energy demand, a hydraulic accumulator is used. The accumulator is sized such that it can be charged by the power supply during the time when the system does not require power from the power supply. This stored energy can then be used for much of the upward vertical motion. Subsequently, the combined energy storage capacity of the accumulator and three way control strategy enable a significant reduction in the hydraulic power supply. The SMSP power supply provides a constant 90 kW of hydraulic power at 13.8 MPa and has a 114 liter accumulator. Each of the vertical heave actuators has a maximum flow rate of 379 l/min (net flow requirement from the power supply is 757 l/min) resulting in a peak power requirement of approximately 174 kW of hydraulic power (almost twice that available from the actual power supply). The combination of the storage capacity of the accumulator and the dwell time available during downward motion clearly provides significant reduction in the sizing of the hydraulic power supply which impacts space requirements as well as cost. While using an accumulator to store energy is fairly common, using it in a motion controlled system with servo valves that allows significant variation in system pressure is not common.

2.5 Controls Outline

We pointed out previously that, as a result of the design process for reducing the overall power consumption, the heave cylinders exhibited a relatively low closed-loop stiffness. Acceleration feedback in the

controller design will be shown in the following sections to overcome this limitation. Furthermore, the mechanical coupling between the two heave cylinders causes the system dynamics to be tightly coupled and a relatively simple transformation will be shown to decouple the system, thereby allowing acceleration feedback to be readily applied. Finally, because gravity is used in lowering the platform to reduce the energy consumption, the system pressure has to be biased to aid in the linearization of the plant.

3 Acceleration Feedback

3.1 Purpose

By placing the main heave actuators in tension instead of compression, the system requires significantly lower rod cross-section which is good in terms of the system's energy requirements (smaller actuator, lower flow rate) but is detrimental in terms of the system stiffness, open-loop bandwidth and subsequently control. The stiffness of a hydraulic actuator is approximately (ignoring the fluid in the lines) the same as a column of fluid stiffness ($A\beta/L$) where A is the piston cross-section, β is the effective fluid's bulk modulus (generally ~690 MPa) and L is the actuator's length. A hydraulic actuator is generally characterized as a lightly damped, type one, third-order system (Merritt, 1967) such as that shown in Fig. 5, where x_v is the servo valve equivalent spool position, K_q is the flow gain, ω_h is the hydraulic system natural frequency, δ_h is the hydraulic system damping ratio, A is the cylinder cross sectional area, and x is the actuator position.

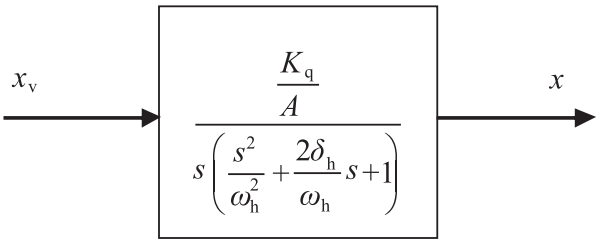

Fig. 5: *Hydraulic actuator model with mass load*

Actually the input to the servo valve controller is a voltage proportional to the orifice opening. This voltage gain is included in the K_q flow gain term. To increase the damping ratio, acceleration feedback, K_a, is commonly utilized, which effectively increases the damping ratio to a value

$$\bar{\delta}_h = \delta_h + \frac{\omega_h K_q K_a}{2A} \quad (1)$$

as can be seen in Fig. 6 and 7. Even when an external force is applied to the actuator model, acceleration feedback will always increase the effective damping ratio of a hydraulic system and is similar to velocity feedback applied to an electric motor.

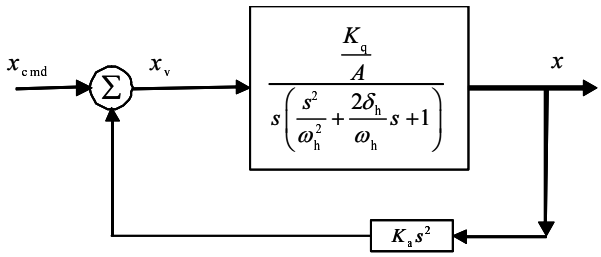

Fig. 6: *Hydraulic actuator model with acceleration feedback*

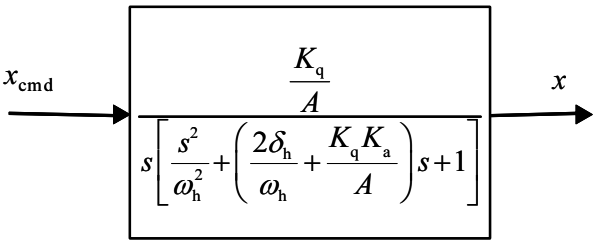

Fig. 7a: *Equivalent hydraulic actuator model with acceleration feedback*

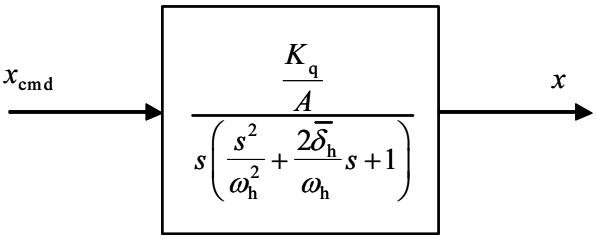

Fig. 7b: *Simplified hydraulic actuator model with acceleration feedback*

We conducted a series of swept sinusoids individually to each mast (before the table was connected) along with varying the joint payload (from 0 to 22 kN) and the position (between upper and lower limits). The damping ratio, δ_h, varied from 0.08 to 0.20 and the natural frequency, ω_h, varied from 5 to 8 Hz (which is roughly the value that was calculated in the previous section). While the system's open-loop bandwidth was more than an order of magnitude greater than our required closed-loop bandwidth (0.2 to 0.5 Hz), the low damping ratio made it difficult to achieve smooth motion, especially when the system changed direction. Also, there was a desire to do time scaling of the motion profile to effectively increase the acceleration forces by a factor of 4, which means that the closed loop bandwidth of the system has to be up to 1 Hz (i.e., 2 × 0.5 Hz). As a rule of thumb (see p. 240 of Merritt), the effective closed loop bandwidth for a simple proportional position controller is approximately $2\delta_h\omega_h$, which means that there is a potential problem in hitting the 1 Hz value (i.e., 2 x 0.08 x 5 = 0.8 Hz).

Acceleration feedback on the two masts was utilized to increase system damping on the hydraulic system and thereby effectively increase the closed-loop bandwidth. Figure 8 shows the joint tracking of just one heave cylinder with an input drive at 0.2 Hz and a 44 kN vertically driven payload. This exceptionally good tracking accuracy was found to be more than adequate for the simulation of ship motion.

3.2 Torsional Dynamic Coupling

Because of the rigid mechanical connection of the pitch-heave cylinders to the platform table (to reduce energy consumption), a high frequency oscillation was found to occur through this mechanical coupling. This high frequency (~16 Hz) vibration was picked up by the accelerometers and is displayed in Fig. 9. The two masts on the SMSP are fundamentally a pair of parallel springs coupling a rigid table as shown in Fig. 10, where x_1 and x_2 are the left and right heave cylinder displacements. The acceleration feedback only resolves the fundamental mode of vibration. However, there is also a pitch mode of vibration (~16 Hz) that has to be dissipated by the joint controllers.

This pitching degree of freedom actually provides a second mode of vibration, the torsional mode, θ.

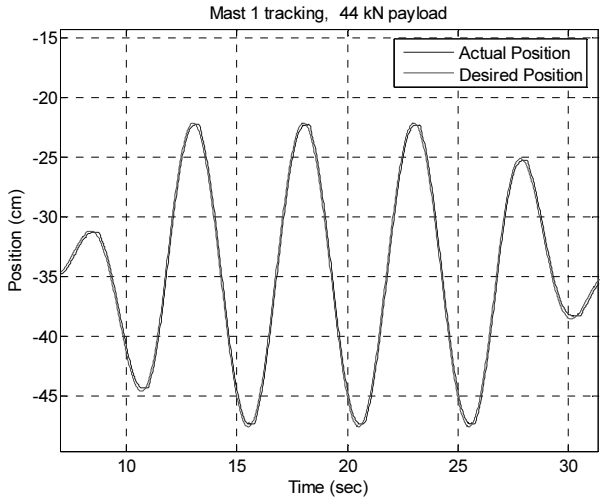

Fig. 8: *Mast tracking*

Subsequently, in Cartesian space, there is one mode of vibration at approximately 5 to 8 Hz associated with the translation degree of freedom and a second mode of vibration at approximately 16 Hz associated with the torsional degree of freedom. Applying the small angle approximation (pitch angle will always be small), the simplified mechanical dynamic model of the system is

$$\begin{bmatrix} \left(\frac{m}{4}+\frac{J}{L^2}\right) & \left(\frac{m}{4}-\frac{J}{L^2}\right) \\ \left(\frac{m}{4}-\frac{J}{L^2}\right) & \left(\frac{m}{4}+\frac{J}{L^2}\right) \end{bmatrix} \begin{Bmatrix} \ddot{x}_1 \\ \ddot{x}_2 \end{Bmatrix} = \begin{Bmatrix} F_1 \\ F_2 \end{Bmatrix} \tag{2}$$

or

$$s^2 \begin{bmatrix} \alpha & \delta \\ \delta & \alpha \end{bmatrix} \begin{Bmatrix} x_1 \\ x_2 \end{Bmatrix} = \begin{Bmatrix} F_1 \\ F_2 \end{Bmatrix}$$

with

$$\alpha = \frac{m}{4}+\frac{J}{L^2} \text{ and } \delta = \frac{m}{4}-\frac{J}{L^2}$$

where F_1 and F_2 are the left and right heave cylinder forces, respectively, and m and J are the effective system mass and inertia of the system.

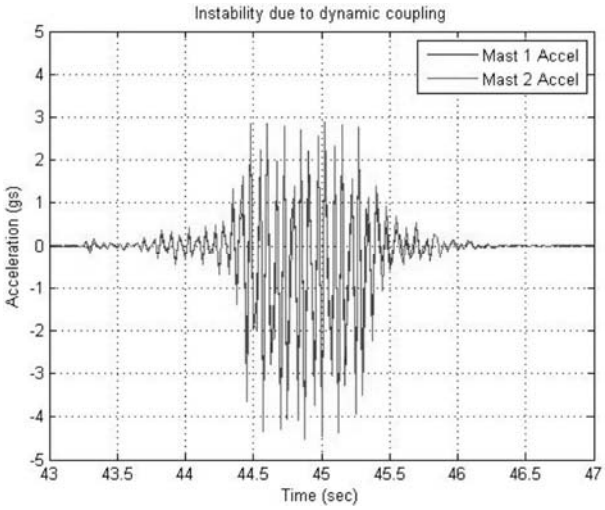

Fig. 9: *Instability due to mast coupling*

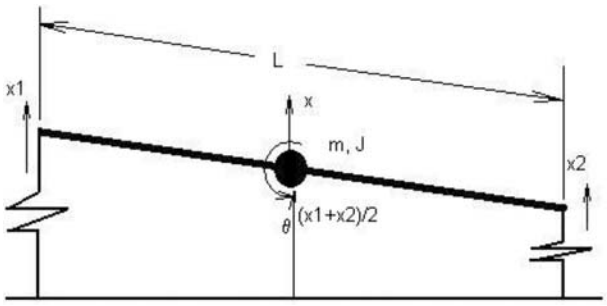

Fig. 10: *Simplified model of coupled masts (pitch and heave)*

The right and left cylinders are identical (A is the same for both). The forces on the two cylinders are proportional to the pressure and cylinder cross sectional area.

$$\begin{aligned} F_1 &= P_1 A \\ F_2 &= P_2 A \end{aligned} \tag{3}$$

From the valve flow and fluid continuity relationship for each valve and cylinder (Merritt, 1967), the flow relationships are:

$$\begin{aligned} Q_1 &= K_q x_{v1} - K_p P_1 \\ &= A\dot{x}_1 + \frac{V_1}{\beta}\dot{P}_1 + C_{ep} P_1 \end{aligned} \tag{4}$$

and

$$\begin{aligned} Q_2 &= K_q x_{v2} - K_p P_2 \\ &= A\dot{x}_2 + \frac{V_2}{\beta}\dot{P}_2 + C_{ep} P_2 \end{aligned}$$

Where Q_1 and Q_2 are the left and right heave valve flows. One can rearrange Eq. 4 and substitute Eq. 3 for a force expression for the actuators as a function of the valve command and cylinder displacement:

$$B(s)\begin{Bmatrix} F_1 \\ F_2 \end{Bmatrix} + As\begin{Bmatrix} x_1 \\ x_2 \end{Bmatrix} = K_q \begin{Bmatrix} x_{v1} \\ x_{v2} \end{Bmatrix} \tag{5}$$

where

$$B(s) = \frac{V}{A\beta}s + \frac{C_{ep}+K_p}{A}$$

and we have assumed that the two cylinders have similar volumes of fluid (V_1 and V_2 are approximately equal to V again due to the small pitch angle). One can now substitute the actuator forces back into the dynamic equations of motion, Eq. 2, and arrange for an input/output relationship

$$\begin{Bmatrix} x_1 \\ x_2 \end{Bmatrix} = \frac{K_q}{s\left[s^2B^2(s)\left(\alpha^2-\delta^2\right)+2s\alpha B(s)+A^2\right]} \cdot \begin{bmatrix} \left(s\alpha B(s)+A\right) & -s\delta B(s) \\ -s\delta \mathrm{B(s)} & \left(s\alpha B(s)+A\right) \end{bmatrix} \begin{Bmatrix} x_{v1} \\ x_{v2} \end{Bmatrix} \tag{6}$$

Subsequently, when connecting the two masts, the system exhibits significant coupling. If acceleration feedback is applied on a joint by joint basis, its intended results are masked by the oscillation that results from the mast mechanical coupling (see Fig. 9). To remedy the problem, a simple MIMO controller based on the Cartesian degrees of freedom was developed. A heave compensator was designed to address the lightly damped poles of the first mode of vibration and a pitch compensator was designed to address the lightly damped poles of the torsional mode of vibration. Assuming small pitch angles, the relationship between the mast positions, x_1 and x_2, and the displacement of the center of the table, x and θ, as shown in Fig. 10, is:

$$\begin{Bmatrix} x \\ \theta \end{Bmatrix} = \begin{bmatrix} 1/2 & 1/2 \\ 1/L & -1/L \end{bmatrix} \begin{Bmatrix} x_1 \\ x_2 \end{Bmatrix} \tag{7}$$

Likewise, the inverse transformation to map the joint commands to the Cartesian space was utilized:

$$\begin{Bmatrix} x_{v1} \\ x_{v2} \end{Bmatrix} = \begin{bmatrix} 1 & L/2 \\ 1 & -L/2 \end{bmatrix} \begin{Bmatrix} u_x \\ u_\theta \end{Bmatrix} \tag{8}$$

Substitution of Eq. 7 and 8 into Eq. 6 decouples the dynamics and produces a similar set of dynamics used for the single degree of freedom case:

$$\begin{Bmatrix} x \\ \theta \end{Bmatrix} = \frac{K_q}{s\left[s^2B^2(s)\left(\alpha^2-\delta^2\right)+2s\alpha B(s)+A^2\right]} \cdot \begin{bmatrix} \left(s\alpha B(s)(\alpha-\delta)+A\right) & 0 \\ 0 & sB(s)(\alpha+\delta)+A \end{bmatrix} \begin{Bmatrix} u_x \\ u_\theta \end{Bmatrix} \tag{9}$$

Because of the obvious common factors in the numerator and denominator, further simplifications are possible:

$$\begin{Bmatrix} x \\ \theta \end{Bmatrix} = \begin{bmatrix} \dfrac{\frac{K_q}{A}}{s\left[sB(s)\frac{m}{2A}+1\right]} & 0 \\ 0 & \dfrac{\frac{K_q}{A}}{s\left[sB(s)\frac{J}{2AL^2}+1\right]} \end{bmatrix} \begin{Bmatrix} u_x \\ u_\theta \end{Bmatrix}$$

or

$$= \begin{bmatrix} \dfrac{\frac{K_q}{A}}{s\left(\frac{s^2}{\omega_{hx}^2}+\frac{2\delta_x}{\omega_{hx}}s+1\right)} & 0 \\ 0 & \dfrac{\frac{K_q}{A}}{s\left(\frac{s^2}{\omega_{h\theta}^2}+\frac{2\delta_\theta}{\omega_{h\theta}}s+1\right)} \end{bmatrix} \begin{Bmatrix} u_x \\ u_\theta \end{Bmatrix} \tag{10}$$

where

$$\omega_{hx}=\sqrt{\frac{2\beta A^2}{Vm}},\ \delta_x=\frac{\left(K_p+C_{ep}\right)}{2A}\sqrt{\frac{\beta m}{2v}},\ \omega_{h\theta}=\sqrt{\frac{2\beta A^2L^2}{VJ}}$$

and

$$\delta_\theta=\frac{\left(K_p+C_{ep}\right)}{2A}\sqrt{\frac{\beta J}{2VL^2}}$$

This transformation simplified the problem from a coupled, type 1, 5th order system to two uncoupled type 1, 3rd order systems. As before, acceleration feedback was added to increase the system damping, but the controllers are designed and tuned in the above Cartesian space, significantly simplifying the problem. The Cartesian controllers are simple lag compensators with acceleration feedback.

$$\begin{aligned} u_x &= \frac{K_p}{\left(\frac{s}{\omega_{pc}}+1\right)}\left(x_d-x\right)-K_p^a\ddot{x} \\ u_\theta &= \frac{K_\theta}{\left(\frac{s}{\omega_{\theta c}}+1\right)}\left(\theta_d-\theta\right)-K_\theta^a\ddot{\theta} \end{aligned} \tag{11}$$

The acceleration feedback gains, K_p^a and K_θ^a are based on a desired damping ratio of 0.7. The DC gains, K_p and K_θ, and the lag poles, ω_{pc} and $\omega_{\theta c}$ are synthesized using MathWorks' SISO toolbox by trial and error. Based on the range of natural frequencies and damping ratios measured during open loop impulse tests on the heave and pitch, a series of plants serve as the input to the SISO tool, and the controllers are based on a gain margin of 10 dB and phase margin of 60°.

4 Bias Setting

By exploiting gravity to help with the downward motion, the flow control servo valve is utilized only on one side of the heave actuator as shown in Fig. 4. There is a subtle problem with the DC plant flow gain (i.e., K_q). Typically one would like the flow gain of the valve to be as symmetric as possible regardless of the direction of the heave cylinders. Typically open-centered valves are utilized to improve linearity, in the flow gain term, but sacrifices energy because flow is always flowing even when no motion is required. The critical-centered valves were selected to minimize energy loss. In an attempt to balance

the flow through the valve regardless of whether the pump or gravity is the primary energy source, it will be shown that the system pressure has to be approximately equal to the gravity and acceleration load on the heave cylinders.

From Fig. 4, the cylinder motion based on fluid continuity and ignoring fluid compressibility is

$$A\,\dot{x} = Q_{+} - Q_{-} \tag{12}$$

where

$$Q_{+} = a_{\mathrm{l}} C_{\mathrm{d}} \sqrt{\frac{2P_{\mathrm{s}}}{\rho}} \sqrt{1 - \frac{P}{P_{\mathrm{s}}}}$$

and

$$Q_{-} = a_{\mathrm{l}} C_{\mathrm{d}} \sqrt{\frac{2P_{\mathrm{s}}}{\rho}} \sqrt{\frac{P}{P_{\mathrm{s}}}} \tag{13}$$

The input to the system is the spool displacement, x_{v}, on the servo valve. (Actually, the input to the servo valve controller is a voltage proportional to the orifice opening.) Subsequently, the flow rate going into the cylinder is a function of both the spool displacement, x_{v}, cylinder pressure, P, and supply pressure, P_{s} where C_{d} is the valve discharge coefficient, a_{i}'s terms the effective valve areas that are electronically controlled with area gradient b, and ρ is the hydraulic fluid density. The cylinder velocity can be written as

$$\dot{x} = \begin{cases} \dfrac{C_{\mathrm{d}} b x_{\mathrm{v}}}{A} \sqrt{\dfrac{2P_{\mathrm{s}}}{\rho}} \sqrt{1 - \dfrac{P}{P_{\mathrm{s}}}} & \text{for } x_{\mathrm{v}} \geq 0 \\ \dfrac{C_{\mathrm{d}} b x_{\mathrm{v}}}{A} \sqrt{\dfrac{2P_{\mathrm{s}}}{\rho}} \sqrt{\dfrac{P}{P_{\mathrm{s}}}} & \text{for } x_{\mathrm{v}} < 0 \end{cases} \tag{14}$$

Let $P = P_{\mathrm{s}}/2 + \Delta P$, and after some manipulation:

$$\dot{x} = \frac{C_{\mathrm{d}} b x_{\mathrm{v}}}{A} \sqrt{\frac{P_{\mathrm{s}}}{\rho}} \sqrt{1 + \frac{2|x_{\mathrm{v}}|}{x_{\mathrm{v}}} \frac{\Delta P}{P_{\mathrm{s}}}} \tag{15}$$

The flow gain, K_{q}, is:

$$K_{\mathrm{q}} = \frac{d\left(A\dot{x}\right)}{dx_{\mathrm{v}}} = C_{\mathrm{d}} b \sqrt{\frac{P_{\mathrm{s}}}{\rho}} \sqrt{1 + \frac{2|x_{\mathrm{v}}|}{x_{\mathrm{v}}} \frac{\Delta P}{P_{\mathrm{s}}}} \tag{16}$$

which is approximately

$$K_{\mathrm{q}} \cong C_{\mathrm{d}} b \sqrt{\frac{P_{\mathrm{s}}}{\rho}} \tag{17}$$

when ΔP is close to 0. The important point in this derivation is that the system pressure should be set to overcome the gravitational load (the table weight and load is accurately known) plus the pressure associated with the maximum acceleration force expected (again, well known from the simulation software) before each run. If the pressure is balanced, the flow gain term will be fairly constant during each run. As an example, the table weighs 22 kN and the system is designed for a maximum payload of 22 kN. The pitch motion is relatively low so the two vertical masts will come close to equally sharing the load. Thus, the average load on each actuator will be approximately 22 kN. The maximum vertical acceleration, in either direction, due to the Sea State is about 0.4 g, so each actuator will experience a bias force of 22 kN with a 8.9 kN variation in either direction. To maintain the 22 kN bias force, and since the actuator cross section area is 33 cm^2, the system supply pressure should be set to 9.4 MPa (= (22,000 + 9,000)/0.0033). As a general rule, it is desirable to maintain this load pressure above $P_s/6$ to ensure the system does not cavitate. By following this simple guideline regarding the selection of the actuator cross section and supply pressure, one can ensure that the valve and actuator will operate in a near symmetrical state. The advantage is then that the control and tracking will be symmetric. Since the payload is known and the motion profile is known before the simulator is started, the supply pressure was reduced or increased accordingly.

5 Tracking Results

Figures 11 and 12 display the resulting joint tracking for the two masts. Just as important, Fig. 13 displays the joint acceleration for both masts. It is clear that the system does not exhibit any of the higher frequency vibration that was present with the coupled system. There is still a minor vibration that occurs when the system changes direction. This is attributed to the nonlinear friction in the actuators but is small enough to be considered acceptable in terms of the system's performance.

Figures 14 and 15 show the tracking in the Cartesian space.

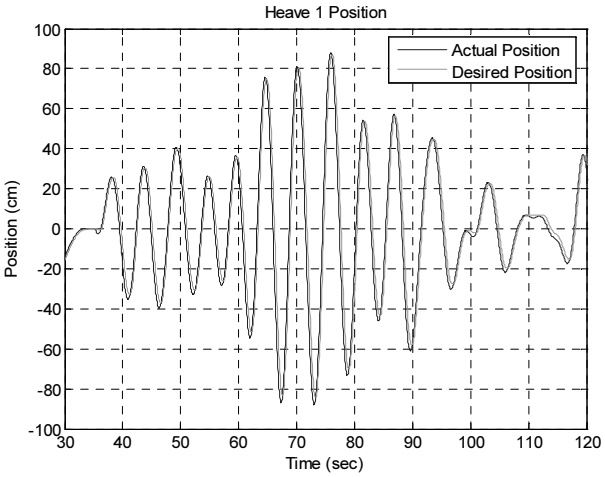

Fig. 11: *Heave cylinder 1 tracking*

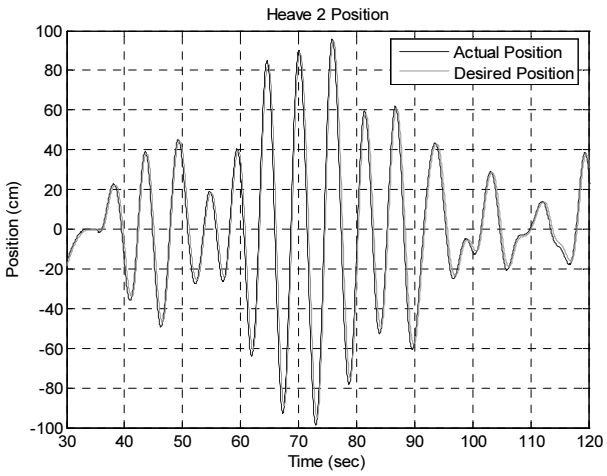

Fig. 12: *Heave cylinder 2 tracking*

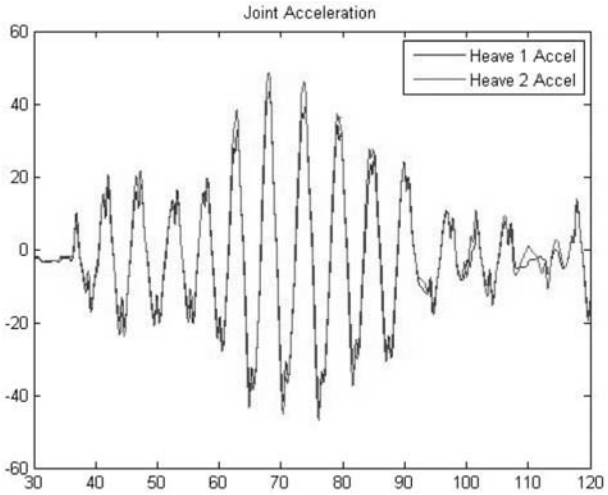

Fig. 13: *Heave 1 and 2 acceleration*

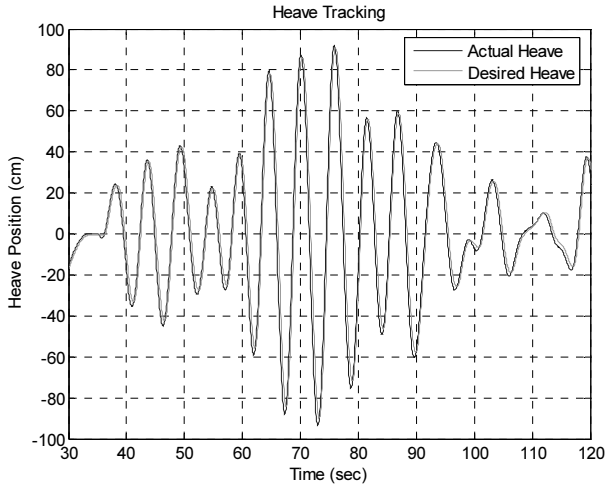

Fig. 14: *Heave tracking*

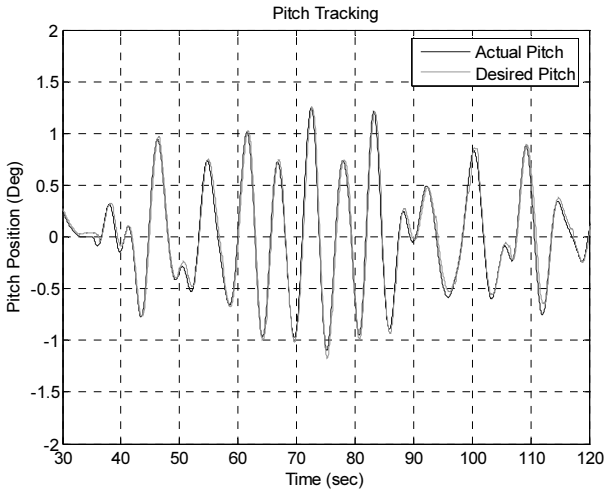

Fig. 15: *Pitch tracking*

For completeness, the tracking for the remaining degrees of freedom in Figs 16 through 18 are shown and display excellent tracking accuracy.

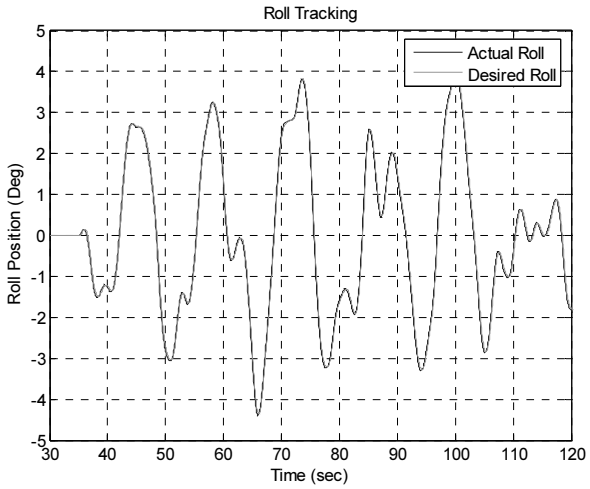

Fig. 16: *Roll tracking*

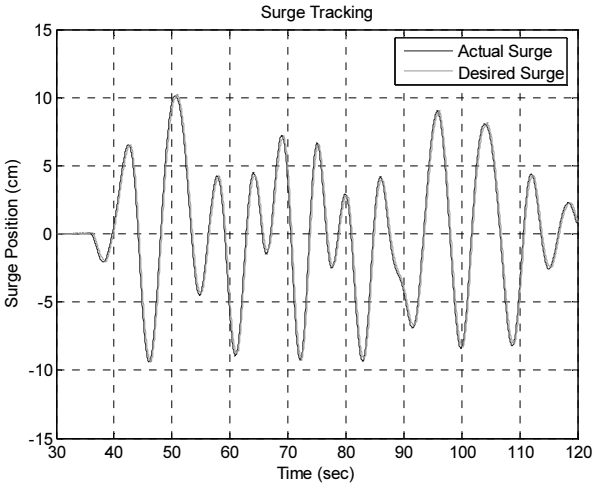

Fig. 17: *Surge tracking*

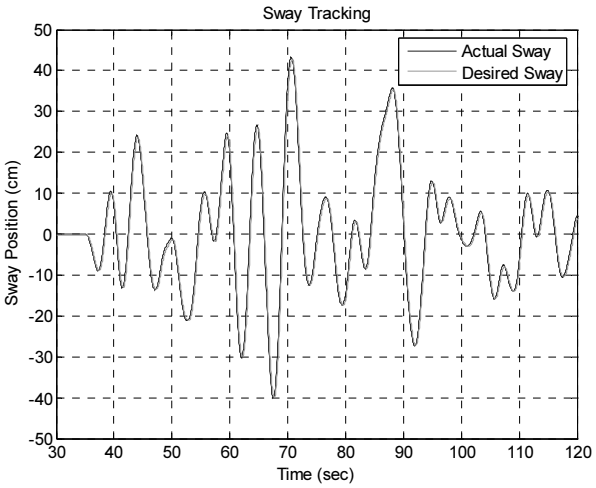

Fig. 18: *Sway tracking*

6 Conclusions

This article has described the design and control of a five degree of freedom ship motion simulation platform. While the original motivation for this work was

directed at developing a facility to test future naval robotic devices, the design and control of the system revealed some interesting challenges associated with large-scale electro-hydraulic systems. Typical large-scale hydraulic systems generally pay little consideration to energy efficiency. As a result, power supplies and actuation components can be significantly oversized. A key point illustrated in this paper is that the combination of energy storage through accumulators coupled with strategic design and controls decisions can have a profound impact on the power requirements. However, there are obviously some penalties for this reduction in available power. In the case discussed in this paper, the system's stiffness and subsequent natural frequency were significantly lower than other systems of comparable sizes. Traditional lag compensators with acceleration feedback can achieve relatively high closed loop bandwidths, but coupling between the joints can significantly limit performance. We demonstrated a simple approach, based on designing the system's controller in the Cartesian space, which significantly simplified the synthesis and tuning of the system's controllers. The primary point of this paper is that there are significant opportunities for improving energy efficiency in electrohydraulic systems.

Acknowledgements

The authors would like to acknowledge the support of Dr. Teresa McMullen and Dr. Geoff Main. This work was performed under Interagency Agreements No. 1866-Q356-A1 and 1866-S508-A1 between the U.S. Department of Energy and the Office of Naval Research and under Work For Other Agreement No. ERD-04-2368 between UT-Battelle, LLC and the Advanced Technology Institute.

References

Lee, W., **Kim, J.** and **Cho, J.** 1998. A driving simulator as a virtual reality tool. *Proc. IEEE Intl. Conf. on Robotics and Automation*, pp. 71-76.

Li, D. and **Salcudean, S.**. 1997. Modeling, simulation and control of a hydraulic stewart platform. *Proc. IEEE Intl. Conf. on Robotics and Automation*, pp. 3360-3366.

Love, L., **Jansen, J.**, and **Pin, F.** 2004. On the modelling of robots operating on ships. *Proc. 2004 IEEE Intl. Conf. on Robotics and Automation.*

Merritt, H. E., 1967. *Hydraulic Control Systems.* John Wiley & Sons.

Tseng, S., **Hu**, **S.**, and **Shaw**, **J.** 2005. Control and motion cues generation of Stewart platform with a DSP based controller. *Proc. IEEE Intl. Conf. on Mechatronics*, pp. 96-101.

Nomenclature

A	cylinder area	[m^2]
C_d	discharge coefficient	[-]
C_{ep}	external leakage coefficient	[m^3/s Pa]
F_i	heave cylinder force	[N]
J	platform inertia	[kg-m^2]
K_a	acceleration feedback gain	[m/s^2]
K_p	valve pressure gain	[m^3/s Pa]
K_q	valve flow gain	[m^2/s]
L	platform length	[m]
m	platform mass	[kg]
P	cylinder pressure	[Pa]
s	Laplace differential operator	[s^{-1}]
u	Cartesian controller	[either m or rad]
x	platform linear displacement from center of mass	[m]
x_i	heave cylinder displacement	[m]
x_v	valve displacement	[m]
x_{cmd}	commanded position	[m]
α	$= m/4 + J/L^2$	[kg]
β	effective fluid bulk modulus	[Pa]
θ	platform angular rotation, pitch, from center of mass	[rad]
ρ	fluid density	[-]
δ_h	hydraulic damping ratio	[kg/m^3]
$\overline{\delta}_h$	equivalent hydraulic damping ratio	[-]
δ	$= m/4 - J/L^2$	[kg]
ω_h	hydraulic undamped natural frequency	[rad/sec]
1	left heave cylinder	
2	right heave cylinder	
s	supply	
x	displacement	
θ	pitch	

John F. Jansen
received the B.S.E.E. and M.S.E.E. degrees from the University of Florida (‘77 and ’79), and the Ph.D. from Georgia Institute of Technology (’85). He is a Distinguished R&D Staff Member at ORNL for the Robotics and Energetic Systems Group Systems Division at Oak Ridge National Laboratory. His research interest are in the design and controls of advanced electro-mechanical and electro-hydraulic systems.

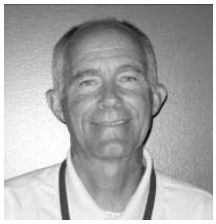

Randall F. Lind
has been a practicing mechanical engineer since 1976 and has developed and designed automation, actuation, mobility and sensor systems for industrial and military applications. He holds a BS degree from the University of Illinois and a MS degree from the University of Tennessee in mechanical engineering. His current interests include construction automation and miniature hydraulics.

Dr. Lonnie Love
is a Distinguished Research Scientist at ORNL and has been in the Robotics and Energetic Systems Group since 1995. His Ph.D. (1995) in Mechanical Engineering is from the Georgia Institute of Technology. His current research interests include the design and control of fluid powered systems, mesofluidics and nanofermentation for the large scale synthesis of nanomaterials.

Peter Lloyd
has a Bachelor of Science in Mechanical Engineering from the U.S. Naval Academy (’79) and a Master of Science in Electrical Engineering from the Naval Postgraduate School (’89) and has been a Development Engineer at the Oak Ridge National Laboratory for 17 years.

John Rowe
has a BS in Engineering Physics from the University of Oklahoma and an MS in Electrical Engineering from the University of Tennessee. He has been a Development Engineer for 33 years, but has been at the Oak Ridge National Laboratory for the past 26 years developing control system hardware and software.

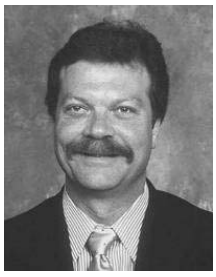

Dr. François G. Pin
is a Corporate Fellow and the Group Leader of the Robotics and Energetic Systems Group at the Oak Ridge National Laboratory (ORNL). His M.S. (1978) and Ph.D. (1982) in Mechanical Engineering and Aerospace Sciences are from the University of Rochester, New York. His current research work includes methodology development for Robotic Mobility and Manipulation Systems, and Intelligent Machines.